Two-phase modelling of air bubbles in ice cream

Problem presented by

Danny Keenan

Unilever Research

Problem statement

Ice cream is essentially a foam consisting of air bubbles dispersed in a mixture of fat, water and ice crystals. The air fraction is typically around 50% by volume, and this is crucial for the product to have the consistency and texture desired by customers. A common manufacturing method involves mixing the air and other ingredients under high pressure before discharging the product to atmospheric pressure for further processing. As the pressure is released, air may escape from the foam into the atmosphere. The Study Group was asked to quantify this air loss and to predict how it might depend on, for example, the rheological properties of the foam mixture, the bubble size distribution and the rate at which the pressure is released.

Study Group contributors

David Allwright (Smith Institute)
Chris Breward (University of Oxford)
John Fozard (University of Oxford)
Peter Howell (University of Oxford)
Sam Howison (University of Oxford)
Mark Muldoon (UMIST)
John Ockendon (University of Oxford)
James Parrott (University of Bristol)
Colin Please (University of Southampton)
Chris Poole (University of Oxford)
Gordon White (University of Oxford)
Eddie Wilson (University of Bristol)

Report prepared by

Peter Howell (University of Oxford)
Mark Muldoon (UMIST)

1   Introduction

Ice cream is essentially a foam consisting of air bubbles dispersed in a mixture of fat, water and ice crystals. The air fraction is typically around 50% by volume, and this is crucial for the product to have the consistency and texture desired by customers. A common manufacturing method involves mixing the air and other ingredients under high pressure (4–5 atmospheres) before discharging the product to atmospheric pressure for further processing. As the pressure is released, air may escape from the foam into the atmosphere, resulting in a lower air fraction in the final product than in the mixer. Such effects can also occur when ice cream is de-pressurised below atmospheric pressure and may cause degradation if the product is transported at high altitude. The aim of this study is to quantify this air loss and to predict how it might depend on, for example, the rheological properties of the foam mixture, the bubble size distribution and the rate at which the pressure is released.

To investigate this phenomenon, the following experiment has been performed at Unilever Colworth. A small sample of ice cream is pressurised up to around five atmospheres, and the pressure is then released over a few seconds. This causes the trapped bubbles to expand, following Boyle's law, and thus the whole sample expands. It is observed, however, that this global expansion is significantly less than Boyle's law would predict, indicating that up to 10% of the air has escaped from the sample during the de-pressurisation. This conclusion is supported by anecdotal evidence that small "volcanic eruptions", accompanied by popping sounds, can sometimes be detected on the surface of the ice-cream. It is worth noting, though, that the air loss is inferred from measurements using Archimedes' principle, so the 10% figure may not be particularly accurate.

We adopt two alternative approaches to the problem. The first is to model the expansion of the foam as a two-phase flow, with air bubbles expanding in a deformable matrix. This allows us to predict the pressure distribution inside the sample. The mismatch between the internal and external pressures drives a net flow of air out of the sample; this flow is localised in a boundary layer at the edge of the sample.

In the second approach, we consider a random distribution of spherical bubbles of a given radius r. The aim here is to determine how many of the bubbles intersect and form "chains" that connect to the edge of the sample. This gives an estimate of the amount of air that is likely to escape from such chains as the sample expands and r increases.

2   Two-phase model

2.1   Basic equations

We model the ice cream as consisting of two phases: a deformable matrix (itself comprising a mixture of water, fat and ice crystals) and air bubbles. Here we present, with brief motivation, the basic averaged equations governing the motion of these two phases; a more detailed derivation may be found in Appendix A. The volume fraction of air is denoted by α, so the volume fraction of matrix is $(1 - \alpha)$. The air is compressible, with variable density ρ, while the matrix is assumed to be incompressible, so that

conservation of mass for the two phases gives

$$(\rho\alpha)_t + \boldsymbol{\nabla} \cdot (\rho\alpha\boldsymbol{u}_a) = 0, \tag{1}$$

$$-\alpha_t + \boldsymbol{\nabla} \cdot \left((1-\alpha)\boldsymbol{u}_m\right) = 0, \tag{2}$$

where $\boldsymbol{u}_a$ and $\boldsymbol{u}_m$ are the (ensemble-averaged) velocities of the air and matrix respectively.

The expansion of the ice cream is assumed to be slow enough for inertial effects to be negligible. Thus the air pressure p_a satisfies

$$\alpha\boldsymbol{\nabla}p_a = \boldsymbol{D}, \tag{3}$$

where $\boldsymbol{D}$ is the interfacial drag exerted on the air by the matrix. The matrix has a pressure p_m and, unlike the air, a non-negligible deviatoric stress tensor $\boldsymbol{\tau}$. Then, if γ is the surface tension of the air-matrix interface, whose average curvature κ is assumed to be a smoothly varying function, then a stress balance on the whole air-matrix mixture leads to

$$\boldsymbol{\nabla}p_a = \boldsymbol{\nabla} \cdot \left((1-\alpha)(\boldsymbol{\tau} - \tau_n\boldsymbol{I})\right) + \gamma(1-\alpha)\boldsymbol{\nabla}\kappa, \tag{4}$$

where the interfacially-averaged normal deviatoric stress is defined by

$$-\tau_n = p_a - p_m - \gamma\kappa.$$

Finally, the pressure and density of the air are assumed to satisfy the gas law

$$p_a = \rho RT,$$

with constant temperature T and gas constant R.

2.2 Constitutive relations

To close the model, we need constitutive relations for $\boldsymbol{\tau}$, τ_n, κ and $\boldsymbol{D}$. We model the matrix as a power-law shear-thinning fluid, viz

$$\boldsymbol{\tau} = \eta\left[\boldsymbol{\nabla}\boldsymbol{u}_m + (\boldsymbol{\nabla}\boldsymbol{u}_m)^T\right],$$

$$\eta = \eta_0\left[\tfrac{1}{2}\left(\boldsymbol{\nabla}\boldsymbol{u}_m + (\boldsymbol{\nabla}\boldsymbol{u}_m)^T\right) : \left(\boldsymbol{\nabla}\boldsymbol{u}_m + (\boldsymbol{\nabla}\boldsymbol{u}_m)^T\right)\right]^{(n-1)/2}, \tag{5}$$

where typical parameter values are

$$\eta_0 \approx 10^4\,\mathrm{Pa\,s}^n, \quad n \approx 0.6.$$

This also suggests that τ_n should be of the form

$$\tau_n = -\eta_0 f(\alpha)|\boldsymbol{\nabla} \cdot \boldsymbol{u}_m|^{n-1}\boldsymbol{\nabla} \cdot \boldsymbol{u}_m, \tag{6}$$

for some scalar function $f(\alpha)$. Similarly we suppose that κ is a given function of the air fraction:

$$\kappa = \frac{k(\alpha)}{a_0}, \tag{7}$$

where a_0 is a characteristic initial bubble radius.

We initially base our model for the interfacial drag $\boldsymbol{D}$ on Stokes drag:

$$\boldsymbol{D} = \frac{\alpha g(\alpha)\eta}{a^2}(\boldsymbol{u}_a - \boldsymbol{u}_m), \tag{8}$$

where a is a typical bubble radius, which may be estimated by $a = a_0/k(\alpha)$. As shown in Appendix B, if $g(\alpha)$ is chosen appropriately, this law may also take account of the coalescence of neighbouring bubbles at different pressures.

It only remains to specify the functions $f(\alpha)$, $k(\alpha)$ and $g(\alpha)$. This will inevitably involve a combination of inspired guesswork and experimental fitting. We propose some plausible first guesses in Appendix B.

2.3   Nondimensionalisation

We consider a sample of typical dimension L. The external air pressure, initially at p_0, is then varied over a timescale of order t_0. The variables are nondimensionalised as follows:

$$\boldsymbol{x} = L\boldsymbol{x}', \quad t = t_0 t', \quad \boldsymbol{u}_a = \frac{L}{t_0}\boldsymbol{u}_a', \quad \boldsymbol{u}_m = \frac{L}{t_0}\boldsymbol{u}_m',$$

$$p_a = p_0 p_a', \quad \rho = \frac{p_0}{RT}\rho', \quad \eta = \eta_0 t_0^{1-n}\eta'. \tag{9}$$

The nondimensionalised governing equations read (with primes dropped)

$$(\rho\alpha)_t + \boldsymbol{\nabla}\cdot(\rho\alpha\boldsymbol{u}_a) = 0, \tag{10}$$

$$-\alpha_t + \boldsymbol{\nabla}\cdot\left((1-\alpha)\boldsymbol{u}_m\right) = 0, \tag{11}$$

$$p_a = \rho, \tag{12}$$

$$-\delta^2\boldsymbol{\nabla}p_a = \mu\eta g(\alpha)k^2(\alpha)(\boldsymbol{u}_a - \boldsymbol{u}_m), \tag{13}$$

$$\boldsymbol{\nabla}p_a = \mu\boldsymbol{\nabla}\cdot\left[(1-\alpha)\eta\left(\boldsymbol{\nabla}\boldsymbol{u}_m + \boldsymbol{\nabla}\boldsymbol{u}_m^T + f(\alpha)\boldsymbol{\nabla}\cdot\boldsymbol{u}_m\boldsymbol{I}\right)\right]$$
$$+\mu C(1-\alpha)\boldsymbol{\nabla}k(\alpha), \tag{14}$$

$$\eta = \left[\frac{1}{2}\left(\frac{\partial u_i}{\partial x_j} + \frac{\partial u_j}{\partial x_i}\right)^2\right]^{(n-1)/2}, \tag{15}$$

where the remaining dimensionless parameters are

$$\delta = \frac{a_0}{L}, \quad \mu = \frac{\eta_0}{p_0 t_0^n}, \quad C = \frac{\gamma t_0^n}{a_0\eta_0}. \tag{16}$$

In the regimes of interest, where the external pressure is varied by several atmospheres over a few seconds, μ is typically small. This implies that the viscous resistance to deformation is small, so the internal air pressure p_a is, to lowest order, equal to the external pressure $P(t)$. We therefore set $p_a \sim P(t) + \mu p_1 + \ldots$ so the problem reduces to

$$\alpha_t + \boldsymbol{\nabla}\cdot(\alpha\boldsymbol{u}_a) = -\alpha\dot{P}/P, \tag{17}$$

$$-\alpha_t + \boldsymbol{\nabla}\cdot\left((1-\alpha)\boldsymbol{u}_m\right) = 0, \tag{18}$$

$$-\delta^2\boldsymbol{\nabla}p_1 = \eta g(\alpha)k^2(\alpha)(\boldsymbol{u}_a - \boldsymbol{u}_m), \tag{19}$$

$$\boldsymbol{\nabla}p_1 = \boldsymbol{\nabla}\cdot\left[(1-\alpha)\eta\left(\boldsymbol{\nabla}\boldsymbol{u}_m + \boldsymbol{\nabla}\boldsymbol{u}_m^T + f(\alpha)\boldsymbol{\nabla}\cdot\boldsymbol{u}_m\boldsymbol{I}\right)\right]$$
$$+C(1-\alpha)\boldsymbol{\nabla}k(\alpha). \tag{20}$$

Of the remaining parameters, δ—the ratio of a typical bubble radius to the sample size—is certainly small, and we will use this fact below. We have no information about the surface tension γ and so treat C as an order one constant for the moment, although it may well be small too.

2.4 Boundary conditions

To deduce appropriate boundary conditions, it is helpful to write (20) in the form $\boldsymbol{\nabla} \cdot \boldsymbol{\sigma} = \mathbf{0}$, where $\boldsymbol{\sigma}$ is the stress tensor for the whole air-matrix mixture, with components

$$\sigma_{ij} = \left(-p_1 + Cs(\alpha)\right)\delta_{ij} + \eta(1-\alpha)\left(\frac{\partial u_{mi}}{\partial x_j} + \frac{\partial u_{mj}}{\partial x_i} + f(\alpha)\frac{\partial u_{mk}}{\partial x_k}\delta_{ij}\right),$$

where

$$s(\alpha) = -\int_\alpha^1 (1-\alpha)k'(\alpha)\,\mathrm{d}\alpha.$$

The boundary conditions to be imposed on the edge of the sample are, therefore,

$$\boldsymbol{u}_m \cdot \boldsymbol{n} = V_n, \tag{21}$$
$$p_1 = Cs(\alpha), \tag{22}$$
$$\boldsymbol{\sigma} \cdot \boldsymbol{n} = \mathbf{0}. \tag{23}$$

These represent respectively (i) the kinematic boundary condition ($\boldsymbol{n}$ and V_n being the unit normal and normal velocity of the edge), (ii) a stress balance on the air phase, (iii) a stress balance on the mixture as a whole. Note that air may penetrate the edge of the sample, while the matrix may not.

2.5 Isotropic model

Now we take the limit $\delta \to 0$; then (19) implies that the interfacial drag is such that the air bubbles are simply convected with the matrix. We may, therefore, seek a solution in which the whole mixture expands or shrinks isotropically as the outside pressure is varied, that is

$$\alpha = \alpha(t), \quad \boldsymbol{u}_a = \boldsymbol{u}_m = \frac{\dot{V}}{3V}\boldsymbol{x}, \tag{24}$$

where $V(t)$ is the volume of the sample. The equations thus reduce to

$$\dot{\alpha} + \frac{\alpha\dot{V}}{V} = -\frac{\alpha\dot{P}}{P}, \tag{25}$$
$$-\dot{\alpha} + \frac{(1-\alpha)\dot{V}}{V} = 0, \tag{26}$$
$$p_1 = Cs(\alpha) + \eta(1-\alpha)[2 + 3f(\alpha)]\frac{\dot{V}}{3V}, \tag{27}$$
$$\eta = \left(\frac{2}{3}\right)^{(n-1)/2}\left|\frac{\dot{V}}{V}\right|^{n-1}. \tag{28}$$

From these, we find that $P\alpha V$ is constant, which corresponds to *Boyle's law* for the air:

$$P\alpha V \equiv \alpha_0. \qquad (29)$$

Then the air fraction is given in terms of P by

$$\alpha = \frac{\alpha_0}{\alpha_0 + P(1 - \alpha_0)}. \qquad (30)$$

Finally, then, we can write the perturbation to the air pressure as

$$p_1 = Cs(\alpha) + 6^{(n-1)/2}(1 - \alpha)\left(2 + 3f(\alpha)\right)\left|\frac{-\alpha \dot{P}}{3P}\right|^{n-1}\left(\frac{-\alpha \dot{P}}{3P}\right), \qquad (31)$$

where α is given by (30). Notice that the boundary condition $p_1 = Cs(\alpha)$ is *not* satisfied, so this isotropic solution predicts a mismatch between the air pressure in the sample and the external pressure. This indicates the presence of a boundary layer near the edge of the sample where there is significant air flow, that is, where the limit $\delta \to 0$ becomes nonuniform. Notice also that the pressure difference is related to the *rate* at which the external pressure is varied, which suggests that the amount of air loss may likewise be rate-dependent, as observed in the experiments.

2.6   Boundary-layer analysis

Now we examine the boundary layer near the edge of the sample in which there is significant air loss. Suppose the edge is given by $x = l(t)$, where $l \propto V^{1/3}$. Then we rescale locally as follows:

$$x = l(t) + \delta\xi, \quad \boldsymbol{u}_a = \frac{\dot{V}}{3V}\begin{pmatrix} l \\ y \\ z \end{pmatrix} + \delta\boldsymbol{u}_{a1} + \dots, \quad \boldsymbol{u}_m = \frac{\dot{V}}{3V}\begin{pmatrix} l \\ y \\ z \end{pmatrix} + \delta\boldsymbol{u}_{m1} + \dots. \quad (32)$$

We also assume that α is to lowest order a function only of ξ and t. Then the leading-order model in the boundary layer is

$$-\alpha_t + \left((1 - \alpha)u_{m1}\right)_\xi + 2(1 - \alpha)\frac{\dot{V}}{3V} = 0, \qquad (33)$$

$$\frac{2\dot{V}}{3V} + \left(\alpha u_{a1} + (1 - \alpha)u_{m1}\right)_\xi = -\frac{\alpha \dot{P}}{P}, \qquad (34)$$

$$-p_{1\xi} = \eta g(\alpha)k^2(\alpha)\left(u_{a1} - u_{m1}\right), \qquad (35)$$

$$p_1 = Cs(\alpha) + \eta(1 - \alpha)\left(2u_{m1\xi} + f(\alpha)\left[\frac{2\dot{V}}{3V} + u_{m1\xi}\right]\right), \qquad (36)$$

$$\eta = \left[2\left(\frac{2\dot{V}^2}{9V^2} + u_{m1\xi}^2\right)\right]^{(n-1)/2}. \qquad (37)$$

Here, the expansion rate is

$$\frac{\dot{V}}{3V} = -\frac{\dot{P}}{3P}\alpha_\infty(t),$$

where the air fraction "at infinity" (*i.e.* inside the sample) is given by (30):

$$\alpha_\infty = \frac{\alpha_0}{\alpha_0 + P(1 - \alpha_0)}.$$

Thus, in the boundary layer, the evolution of α is given by the hyperbolic equation

$$\alpha_t + u_{m1}\alpha_\xi = (1 - \alpha)\left(u_{m1\xi} + \frac{2\dot{V}}{3V}\right), \tag{38}$$

while the matrix velocity u_{m1} satisfies the third-order quasi-steady equation

$$\left\{u_{m1} - \frac{\alpha}{\eta g k^2}\left[Cs + \eta(1 - \alpha)\left(2f\frac{\dot{V}}{V} + (2 + f)u_{m1\xi}\right)\right]_\xi\right\}_\xi = -\frac{\alpha\dot{P}}{P} - \frac{2\dot{V}}{3V}. \tag{39}$$

The boundary conditions come from matching with the isotropically expanding solution at infinity,

$$u_{m1} \sim \frac{\dot{V}}{3V}\xi + o(1) \quad \text{as} \quad \xi \to -\infty, \tag{40}$$

and the stress balance and kinematic boundary condition,

$$u_{m1\xi} = -\frac{2f\dot{V}}{3V(2 + f)}, \quad u_{m1} = \dot{X} \quad \text{on} \quad \xi = X(t), \tag{41}$$

where the free boundary of the sample is given by $\xi = X(t)$.

This problem in principle allows us to obtain the air fraction in the boundary layer at the edge of the sample and, thus, to determine the amount of air that is expelled from these boundary layers. It remains to solve the equations numerically using semi-empirical formulae for the functions f, g and k such as those given in Appendix B.

3 Random dispersions of bubbles

Although a careful account of the dynamics of the expanding food-foam must form the basis of any thorough understanding of this problem it proves both entertaining and informative to think about a much simpler problem involving a uniform dispersion of (potentially overlapping) spherical bubbles. To begin with, consider the centres of the bubbles: we take them to have a Poisson distribution with number density N centres per unit volume. That is, we say

$$P(\text{ exactly } k \text{ centres in a volume } v \text{ }) = \frac{(Nv)^k}{k!}e^{-Nv}. \tag{42}$$

We will further imagine that each centre is surrounded by an air-filled spherical void of radius r. Of course, if two centres are sufficiently close (separation $d < 2r$, see Figure 1) their bubble-spheres will overlap and we will take this to mean that both centres are inside a single, larger, oddly-shaped bubble.
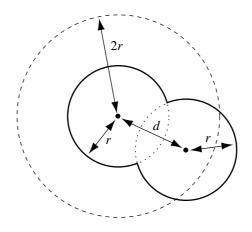
Figure 1: *Two spherical bubbles whose centres are separated by a distance $d < 2r$ merge to form a single, larger bubble.*

3.1 The volume fraction of air

The first question that springs to mind is: "What fraction of the foam's volume is occupied by air?" Let us denote this number as ϕ, the volume fraction of air. Now consider a point somewhere inside the food-foam. The probability that this point lies outside any bubble is, on the one hand, clearly $(1 - \phi)$, the volume fraction of non-air. On the other hand, the point lies outside any bubble if the nearest centre is at least a distance r away. That is, the point lies outside any bubble provided that no centres fall within a ball of radius r around it. So then, using Equation (42),

$$
\begin{aligned}
(1 - \phi) &= P(\text{ randomly chosen point is outside all bubbles }) \\
&= P(\text{ no centres in ball of radius } r) \\
&= e^{-Nv_b},
\end{aligned}
\tag{43}
$$

where N is the number density of bubble centres and $v_b = (4\pi/3)r^3$ is the volume of a bubble.

The quantity Nv_b arises so frequently that we will introduce a notation for it:

$$
\eta = Nv_b = \left(\frac{4\pi}{3}\right)Nr^3.
\tag{44}
$$

Note that once one specifies the volume fraction of air, ϕ, equation (43) fixes the value of η.

3.2 Estimating air loss

Now consider a cube of food-foam whose edges have length L. In this section we will obtain an estimate for the fraction of the cube's bubbles that are connected, via overlap, to the surrounding air. The idea is separately to estimate two quantities: the number of outlets through which air can escape the foam and the fraction of bubbles connected to such outlets.

3.2.1 Number of outlets

Bubbles whose centres lie within a distance r of the walls of the cube will actually pierce the wall and so they provide the outlets through which gas can escape the foam. It is easy to see that the expected number of such outlets is just

$$N\left(L^3 - (L - 2r)^3\right),$$

where the $(L - 2r)^3$ term is the volume of the cube's interior—that part of its volume which is further than r from all of the walls. Under the assumption that $r \ll L$ one can simplify this a bit to find

$$\begin{aligned}
N\left(L^3 - (L - 2r)^3\right) &= N\left(L^3 - (L^3 - 6rL^2 + \cdots)\right) \\
&\approx Nr(6L^2),
\end{aligned} \tag{45}$$

which, given that the cube has six faces, each with area L^2, seems perfectly reasonable. If the foam were a different shape, with surface area A, the expected number of centres within r of the surface would be NrA (assuming still that r is small enough).

3.2.2 Length of bubble chains

Having found the expected number of outlets, one is then prompted to ask how many bubbles are connected to them. Here we will estimate that quantity under the assumption that the network of connected bubbles forms a chain in the sense that each bubble is connected to, at most, two others. Unfortunately one outcome of this analysis is to show that real food-foams—ice cream at room pressure, for example—do not obey this assumption.

Consider first a bubble that is itself an outlet: it may be isolated or it may be connected with other bubbles. The probability of the former case is the same as the probability that the outlet bubble does not overlap any others or, equivalently, that a ball of radius $2r$ around the outlet bubble's centre contains no *other* centres. That is:

$$\begin{aligned}
p_1 \equiv P(\text{ outlet is isolated }) &= P(\text{ no other centres in ball of radius } 2r) \\
&= e^{-8\eta}.
\end{aligned} \tag{46}$$

The quantity $8\eta = 8Nv_b$ that appears in this expression arises because a ball of radius $2r$ has eight times the volume v_b of a ball of radius r.

Now consider the second possibility, that the outlet is not isolated. This happens with probability $(1 - p_1)$. But the chain of bubbles will contain only two members—the outlet and one other—if a ball of radius $2r$ around the second bubble's centre contains no further centres. The probability of this is thus

$$P(\text{ chain of exactly two bubbles }) = (1 - p_1)p_1.$$

The chain of bubbles may, of course, have even more than two members. This happens if a ball of radius $2r$ around the second bubble does contain a further centre, which has probability $1 - p_1$.
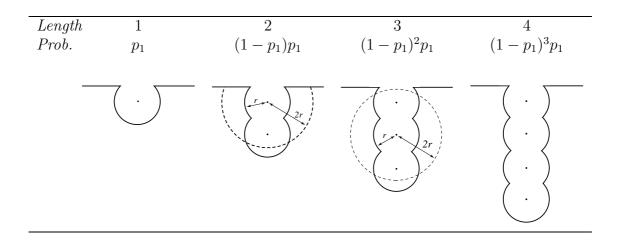
Length	1	2	3	4
Prob.	p_1	$(1-p_1)p_1$	$(1-p_1)^2 p_1$	$(1-p_1)^3 p_1$

Table 1: *Bubble chains of various lengths along with the approximate probabilities of their occurrence: p_1 is defined in equation (46).*

Table 1 summarises these considerations and guides one to write down the following general expression:

$$P(\text{ chain has exactly } k \text{ bubbles }) \;=\; p_1(1-p_1)^{k-1} \quad \text{for } k \geq 1. \tag{47}$$

Armed with this, we can work out the expected length of a chain of bubbles

$$
\begin{aligned}
< \text{length} > \;&=\; \sum_{k=1}^{\infty} k p_1 (1-p_1)^{k-1} \\
&=\; 1/p_1.
\end{aligned}
$$

Multiplying this expected length by the expected number of outlets yields the number of bubbles expected to be connected to the exterior of the cube,

$$< \text{number connected to exterior} > \;=\; (6NrL^2)/p_1$$

and, dividing by NL^3, the total number of bubbles one expects to find in the cube, one finds that the expected fraction ν of bubbles connected to the exterior:

$$\nu \;\equiv\; < \text{fraction connected to exterior} > \;=\; r(6/L)(1/p_1). \tag{48}$$

These are the bubbles whose gas will escape and whose volume will appear as "missing" in Archimedes' principle experiments in which the solvent wets the walls of the bubble tunnels, penetrating to the ends of the chains.

3.2.3 Remarks

1. If one wishes to consider air loss from some solid other than a cube with volume L^3 one should replace the factor $(6/L)$ in Equation (48) with the surface-area-to-volume ratio for the solid in question.

2. Eddie Wilson pointed out that this analysis depends crucially on the assumption that chains of bubbles don't branch. It also ignores other geometric constraints

relating to the boundary of the foam volume: centres within r of the boundary have already been counted as outlet points (and should not be counted again). Also if a centre c is within r of the boundary, then the sphere of radius $2r$ about c does not lie wholly within the foam, which again invalidates the calculation of p_1 above.

3. After the Study Group, Mathew Penrose (Department of Mathematical Sciences, University of Durham) kindly drew our attention to some of the percolation literature relevant to this problem, [5], [6], [7], and [8]. If we just consider the bubble centres away from the boundary of the foam, then they form what is sometimes known as a "Poisson blob model" in percolation theory. The spheres centred on these points form connected 'clusters', containing $k \geq 1$ centres. There will be a certain critical density N_c above which the expected value of k is infinite: this is the threshold at which percolation becomes possible, and we shall assume we are below that threshold. Then [5] describes how to calculate the probability distribution of k, and [7] gives numerical results. In fact [4] derives heuristically our result (47), and [7] compares this with the exact results and concludes that it is a good approximation for η up to about 0.05. The paper [7] also gives the formula (but not numerical results) for the volume of space occupied by clusters of size k. However, this literature does not seem to address our specific question of how much of the volume is connected to the given plane which is the boundary of the foam.

4. The various probabilities that come into this analysis depend only on the parameter η defined in equation (43) and η depends only on the volume fraction of air, ϕ. Plugging in the value $\phi = 0.5$ appropriate for ice cream at room pressure one finds $\eta = \log 2 \approx 0.69$, which is much larger than the threshold mentioned in the previous remark. Therefore, one does *not* expect the bubbles in ice cream to be connected into chains of the sort analysed here, but rather into elaborate networks of extensively branched tunnels: the analysis above does not apply to ice cream. Instead to proceed along these lines one would have to develop the methods of the continuum percolation approach, in order to estimate what volume of space is connected to a given plane per unit area of that plane.

3.3   Simulation

Alongside the probabilistic argument developed above we also did some direct simulations about bubbles in a cube with edges $L = 1$ cm. long. The strategy is similar in outline to the probabilistic argument above in that we first locate the outlets of any tunnels of bubbles, then follow the tunnels back into the body of the cube until they stop. The simulation does not, however, make any assumptions about branching: it simply locates and counts all bubbles that are, via overlap, connected to the cube's exterior. A typical run consists of the following steps:

1. Fix the total number of bubbles N and choose N bubble-centres from a uniform distribution over the cube.

N	Bubble radius r (μm)	Fraction ν of bubbles connected to exterior
12500	286.57	16.48%
25000	227.45	13.88%
50000	180.53	10.94%
100000	143.29	8.69%
200000	113.73	6.80%
400000	90.26	5.44%

Table 2: *Results from simulations of N bubbles in 1 cm. cube. The volume fraction of air is taken to be 0.5 in all these simulations.*

2. Fix the volume fraction of air to be $\phi = 0.5$ and use N as the number density to solve Equation (43) for the radius r of the bubble.

3. Assign a status, initially `Unclassified`, to each bubble.

4. Find all the outlets: those bubbles that lie within r of the walls. Put these points into a list `tips[]`, of the bubbles-to-be examined and change their status to `InTunnels`.

5. For each centre appearing in the `tips[]` list, locate[1] any other centres that lie within a distance $2r$ and, if their status is still `Unclassified`, mark them as `InTunnels` and add then to the list of `tips[]`.

6. Repeat the previous step until `tips[]` is empty.

7. Count the number of centres classified as `InTunnels` and divide by N, then report the fraction of bubbles that are part of tunnels.

Table 2 shows the results of several such simulations: they are modestly encouraging in that when $N \approx 10^4$ they include plausible fractions of bubbles connected to the outside and when $N \approx 5 \times 10^5$ the bubble radius is close to the observed values of 10–100 μm. Unfortunately the nearly-correct bubble fractions occur for rather unrealistically large bubbles and the the nearly-correct bubble radii give rise to rather less air loss than one observes.

3.3.1 Afterword: the effective radius

When we presented the simulations above on the last day of the Study Group Sam Howison suggested that one might allow the bubbles to have an "effective radius" that is somewhat larger than their true radius. His idea was that if a bubble of radius r contained gas at high pressure and was within some distance, call it βr with $\beta > 1$, of the outside wall then it would burst through and create an outlet. That bubble's

---

[1]This process—searching for near neighbours—is the crux of the problem. Direct computation of all pairwise distances between centres is an $O(N^2)$ process and is far too time consuming, but we used an $O(N \log(N))$ algorithm described in a collection of papers about K-d trees assembled in [1].

interior would then equilibrate with the exterior pressure and so bubbles whose surface was within βr of the new outlet's centre would also burst.

Implementing Sam's idea requires only a small modification to the analysis given here: one replaces $2r$ with $(1 + \beta)r$ and 8η with $(1 + \beta)^3\eta$ in the previous section and makes the corresponding changes to the simulations. Table 3 shows results from the modified simulation. The code that produced these results is available from

```
ftp://azure.ma.umist.ac.uk/WWW_Docs/Download/esgi/bubbles.tgz
```

4   Conclusions

We have presented two possible approaches to the modelling of bubble expansion in de-pressurised ice cream. The first is to model the ice cream as a two-phase mixture of air bubbles and deformable matrix. We found that the internal and external air pressures are approximately equal if the expansion rate is reasonably slow. The pressure difference is then given by the *rate* at which the external pressure is varied. Since it is this pressure mismatch that drives air out of the mixture, this supports the experimental evidence that the rate of pressure release plays a crucial role in the loss of air.

The second approach is to distribute spherical bubbles at random then determine how many of them are connected via chains to the edge of the sample. This was estimated both via probability theory and by direct simulation, and the results of the two approaches agree qualitatively. We found that, with realistic bubble sizes and air fractions, the predicted air loss is somewhat lower than that observed in practice. The results may be improved by allowing the bubbles to have an "effective radius", slightly larger than their actual radius.

Both of our approaches predict that most of the air loss occurs at the edge of the sample. This could be tested experimentally by trying samples with different surface-area-to-volume ratios. It would also be interesting to cut open a de-pressurised sample and examine it under the microscope to determine whether there are any noticeable morphological differences between the bulk and edge regions. It was also suggested that tracer gas might be used to get more idea of the gas flow that may be occurring inside, and out of, the sample.

There is plenty more work to be done on this problem. The models presented in §2 still need to be solved numerically so that the predicted air loss may be quantified. More could be done to analyse the statistics produced by the random simulations of §3, and to improve the probabilistic predictions. Ideally, the two approaches of §§2 and 3 should be combined. The random-bubble approach gives information about bubble coalescence that would improve on the *ad hoc* modelling given in Appendix B, while the two-phase approach predicts the pressure distribution in the mixture, which should be related to the "effective radius".

A   Derivation of two-phase model

Here we give a brief derivation of the model equations used in the text. We consider two phases, namely air (denoted by subscript a) dispersed in a "matrix" phase (denoted by

N	β	ν
12500	1.1	17.94%
($r = 286.57\ \mu$m)	1.2	19.70%
	1.3	21.44%
	1.4	23.06%
	1.5	24.78%
25000	1.1	15.26%
($r = 227.45\ \mu$m)	1.2	16.69%
	1.3	18.01%
	1.4	19.39%
	1.5	20.90%
50000	1.1	11.93%
($r = 180.53\ \mu$m)	1.2	13.04%
	1.3	14.15%
	1.4	15.15%
	1.5	16.29%
100000	1.1	9.57%
($r = 180.53\ \mu$m)	1.2	10.41%
	1.3	11.33%
	1.4	12.20%
	1.5	13.06%
200000	1.1	7.48%
($r = 113.73\ \mu$m)	1.2	8.17%
	1.3	8.85%
	1.4	9.52%
	1.5	10.21%
400000	1.1	5.98%
($r = 90.26\ \mu$m)	1.2	6.51%
	1.3	7.06%
	1.4	7.61%
	1.5	8.14%

Table 3: *Fraction of bubbles ν connected to the exterior for simulations with various values of N bubbles (in a 1 cm. cube) and the effective radius β.*

subscript m). Let χ be an indicator function that is equal to 1 in the air phase and 0 in the matrix phase. The air volume fraction is thus given by

$$\alpha = <\chi>,$$

where $<\phi>$ is the *ensemble average* of a quantity ϕ, that is, the average over many different realisations of the problem.[2]. Derivatives are assumed to commute with the averaging process, so that

$$< \frac{\partial \phi}{\partial t} > \equiv \frac{\partial}{\partial t} <\phi>, \quad <\boldsymbol{\nabla}\phi> \equiv \boldsymbol{\nabla} <\phi>$$

and so forth.

Conservation of mass for the air phase implies that

$$\chi\left[\frac{\partial \rho_a}{\partial t} + \boldsymbol{\nabla}\cdot(\rho_a\boldsymbol{u}_a)\right] = 0 \quad \Rightarrow \quad \frac{\partial}{\partial t}(\chi\rho_a) + \boldsymbol{\nabla}\cdot(\chi\rho_a\boldsymbol{u}_a) + \rho_a\left[\frac{\partial\chi}{\partial t} + \boldsymbol{u}_a\cdot\boldsymbol{\nabla}\chi\right] = 0, \quad (49)$$

where ρ_a and $\boldsymbol{u}_a$ are the air density and velocity respectively. The two phases are assumed to be immiscible, so the final term in square brackets is identically zero. Thus, if we define the average air density and velocity by

$$<\chi\rho_a> = \alpha\bar{\rho}_a, \quad <\chi\rho_a\boldsymbol{u}_a> = \alpha\bar{\rho}_a\bar{\boldsymbol{u}}_a,$$

then, by taking the average of (49), we find that

$$\frac{\partial}{\partial t}(\alpha\bar{\rho}_a) + \boldsymbol{\nabla}\cdot(\alpha\bar{\rho}_a\bar{\boldsymbol{u}}_a) = 0. \tag{50}$$

Similarly, for the matrix phase, with density ρ_m and velocity $\boldsymbol{u}_m$, we find

$$\frac{\partial}{\partial t}\Big((1-\alpha)\bar{\rho}_m\Big) + \boldsymbol{\nabla}\cdot\Big((1-\alpha)\bar{\rho}_m\bar{\boldsymbol{u}}_m\Big) = 0, \tag{51}$$

where

$$<(1-\chi)\rho_m> = (1-\alpha)\bar{\rho}_m, \quad <(1-\chi)\rho_m\boldsymbol{u}_m> = (1-\alpha)\bar{\rho}_m\bar{\boldsymbol{u}}_m.$$

Now, if inertia and gravity are negligible, then conservation of momentum for the two phases gives

$$\chi\boldsymbol{\nabla}\cdot\boldsymbol{\sigma}_a = (1-\chi)\boldsymbol{\nabla}\cdot\boldsymbol{\sigma}_m = \boldsymbol{0},$$

where $\boldsymbol{\sigma}_a$ and $\boldsymbol{\sigma}_m$ are the stress tensors in the air and matrix respectively. These may be rearranged to give

$$\boldsymbol{\nabla}\cdot(\chi\boldsymbol{\sigma}_a) - \boldsymbol{\sigma}_a\cdot\boldsymbol{\nabla}\chi = \boldsymbol{\nabla}\cdot\Big((1-\chi)\boldsymbol{\sigma}_m\Big) + \boldsymbol{\sigma}_m\cdot\boldsymbol{\nabla}\chi = \boldsymbol{0}. \tag{52}$$

Recall that the indicator function χ is constant except at the interface between the two phases, where it has a jump of unit magnitude. It follows that $\boldsymbol{\nabla}\chi$ is a delta-function concentrated at the interface, multiplied by the unit normal pointing from the matrix

---

[2]For more details of this averaging, see *e.g.* Drew [2] or Fowler [3, §16.6]

into the air. Hence, continuity of stress at the interface, with surface tension γ and curvature κ gives rise to

$$\boldsymbol{\sigma}_a \cdot \boldsymbol{\nabla}\chi = \boldsymbol{\sigma}_m \cdot \boldsymbol{\nabla}\chi - \gamma\kappa\boldsymbol{\nabla}\chi. \tag{53}$$

We decompose each stress tensor into a pressure p and deviatoric stress $\boldsymbol{\tau}$:

$$\boldsymbol{\sigma}_a = -p\boldsymbol{I} + \boldsymbol{\tau}_a, \quad \boldsymbol{\sigma}_m = -p\boldsymbol{I} + \boldsymbol{\tau}_m.$$

Furthermore, we decompose the deviatoric stress on the interface into its normal and tangential components:

$$\boldsymbol{\tau}_a \cdot \boldsymbol{\nabla}\chi = \tau_{an}\boldsymbol{\nabla}\chi - \boldsymbol{D}_a, \quad \boldsymbol{\tau}_m \cdot \boldsymbol{\nabla}\chi = \tau_{mn}\boldsymbol{\nabla}\chi + \boldsymbol{D}_m.$$

Here $\boldsymbol{D}_a$ and $\boldsymbol{D}_m$ represent respectively the tangential drag on the air due to the matrix and that on the matrix due to the air. By substituting this decomposition into (53), we find that these are equal and opposite:

$$\boldsymbol{D}_a + \boldsymbol{D}_m = \boldsymbol{0},$$

and that the normal stresses are related by

$$-p_{ai} + \tau_{an} = -p_{mi} + \tau_{mn} - \gamma\kappa, \tag{54}$$

where p_{ai} and p_{mi} are the pressures evaluated on the interface.

When all this is substituted into (52), we obtain the following equation for (*e.g.*) the air phase:

$$\boldsymbol{\nabla}(\chi p_a) = \boldsymbol{\nabla} \cdot (\chi\boldsymbol{\tau}_a) + (p_a - \tau_{an})\boldsymbol{\nabla}\chi + \boldsymbol{D}_a.$$

Now this equation is averaged, using the following definitions

$$\alpha\bar{p}_a = <\chi p_a>, \quad \alpha\bar{\boldsymbol{\tau}}_a = <\chi\boldsymbol{\tau}_a>,$$

$$\bar{p}_{ai}\boldsymbol{\nabla}\alpha = <p_a\boldsymbol{\nabla}\chi>, \quad \bar{\tau}_{an}\boldsymbol{\nabla}\alpha = <\tau_{an}\boldsymbol{\nabla}\chi>, \quad \bar{\boldsymbol{D}} = <\boldsymbol{D}_a>,$$

resulting in

$$\boldsymbol{\nabla}(\alpha\bar{p}_a) = \boldsymbol{\nabla} \cdot (\alpha\bar{\boldsymbol{\tau}}_a) + (\bar{p}_{ai} - \bar{\tau}_{an})\boldsymbol{\nabla}\alpha + \bar{\boldsymbol{D}}. \tag{55}$$

Similarly, for the matrix phase we obtain

$$\boldsymbol{\nabla}\Big((1-\alpha)\bar{p}_m\Big) = \boldsymbol{\nabla} \cdot \Big((1-\alpha)\bar{\boldsymbol{\tau}}_m\Big) + (\bar{\tau}_{mn} - \bar{p}_{mi})\boldsymbol{\nabla}\alpha - \bar{\boldsymbol{D}}. \tag{56}$$

The basic equations of motion are (50), (51), (55) and (56). To make further progress, closure assumptions are needed to reduce the number of dependent variables. The first such assumption that we make is that *the interfacial- and bulk-averaged pressures are equal*, that is $\bar{p}_{ai} \equiv \bar{p}_a$ and $\bar{p}_{mi} \equiv \bar{p}_m$. Then (55) and (56) reduce to

$$\alpha\boldsymbol{\nabla}\bar{p}_a = \boldsymbol{\nabla} \cdot (\alpha\bar{\boldsymbol{\tau}}_a) - \tau_{an}\boldsymbol{\nabla}\alpha + \bar{\boldsymbol{D}}, \tag{57}$$

$$(1-\alpha)\boldsymbol{\nabla}\bar{p}_m = \boldsymbol{\nabla} \cdot \Big((1-\alpha)\bar{\boldsymbol{\tau}}_m\Big) + \tau_{mn}\boldsymbol{\nabla}\alpha - \boldsymbol{D}. \tag{58}$$

These may be added to obtain an equation representing net conservation of momentum for the two phases, namely

$$\boldsymbol{\nabla}\bar{p}_a = \boldsymbol{\nabla} \cdot \Big[\alpha\bar{\boldsymbol{\tau}}_a + (1-\alpha)\bar{\boldsymbol{\tau}}_m + (1-\alpha)(\bar{\tau}_{an} - \bar{\tau}_{mn})\boldsymbol{I}\Big] + \gamma(1-\alpha)\boldsymbol{\nabla}\bar{\kappa}, \tag{59}$$

where $\bar{\kappa}$ is the average interface curvature.

The remaining constitutive assumptions depend on the material properties of the air and matrix phases. Since the air is much less viscous than the matrix, we neglect the deviatoric air stresses $\boldsymbol{\tau}_a$ and τ_{an}. The air pressure and density are assumed to satisfy the ideal gas law (at uniform temperature T, with gas constant R), while the matrix is assumed to be incompressible, so that $\rho_m = \text{const}$. The governing equations thus reduce to

$$
\begin{aligned}
(\rho_a \alpha)_t + \boldsymbol{\nabla} \cdot (\rho_a \alpha \boldsymbol{u}_a) &= 0, \\
-\alpha_t + \boldsymbol{\nabla} \cdot \left((1-\alpha) \boldsymbol{u}_m \right) &= 0, \\
\alpha \boldsymbol{\nabla} p_a &= \boldsymbol{D}, \\
\boldsymbol{\nabla} p_a &= \boldsymbol{\nabla} \cdot \left[(1-\alpha) \boldsymbol{\tau}_m - \tau_{mn} \boldsymbol{I} \right] + \gamma (1-\alpha) \kappa, \\
p_a &= \rho_a R T.
\end{aligned}
$$

(with overbars dropped).

B   Possible forms for the functions f, k and g

Here we propose constitutive equations for the three unknown functions $f(\alpha)$, $k(\alpha)$ and $g(\alpha)$ remaining in our model. These are based on a highly simplified picture of reality in which the bubbles occupy a regular cubic lattice. We therefore need only consider a single cubic cell, of diameter ℓ say, containing a bubble of radius a. These are related to the initial bubble radius a_0, and the current and initial air fractions α and α_0, by

$$
\frac{\ell}{a_0} = \left(\frac{4\pi(1-\alpha_0)}{3\alpha_0(1-\alpha)} \right)^{1/3}, \quad \frac{a}{a_0} = \left(\frac{\alpha(1-\alpha_0)}{\alpha_0(1-\alpha)} \right)^{1/3}.
$$

This suggests an interface curvature of the form

$$
k(\alpha) = \frac{a_0}{a} = \left(\frac{\alpha_0(1-\alpha)}{\alpha(1-\alpha_0)} \right)^{1/3}. \tag{60}
$$

The thickness h of the "lamella" between neighbouring bubbles is given by

$$
\frac{h}{a_0} = 2 \left(\frac{1-\alpha_0}{\alpha_0(1-\alpha)} \right)^{1/3} \left[(\pi/6)^{1/3} - \alpha^{1/3} \right].
$$

If a pressure drop Δp is applied across such a lamella, then we might imagine that its likelihood of rupturing is proportional to $\Delta p / (\eta h)$. If the lamella *does* rupture, then there will be a flow of air from the higher pressure bubble to the lower pressure one. The net velocity difference between the two phases arising from such events may thus be expected to take the form

$$
\boldsymbol{u}_a - \boldsymbol{u}_m \propto -\frac{\ell^2 a}{h\eta} \boldsymbol{\nabla} p_a.
$$

This is consistent with (8) if $g(\alpha)$ is proportional to ha/ℓ^2, that is

$$
g(\alpha) = g_0 \alpha^{1/3} \left[(\pi/6)^{1/3} - \alpha^{1/3} \right]. \tag{61}
$$

Notice in particular that $g \to 0$ as $\alpha \to \pi/6$, which is just greater than 50%. If α reaches this critical value, then the bubbles are all connected and, in this idealised model, the matrix ceases to offer any resistance to the air.

Finally, to estimate the function $f(\alpha)$, we consider a spherical bubble in an unbounded region of power-law fluid. Of course, this is probably not very accurate when the air fraction is as high as 50%, but will provide an initial guess at least. The velocity field is of the form

$$\boldsymbol{u} = \frac{a^2 \dot{a}}{r^2} \boldsymbol{e}_r,$$

where r is radial distance from the centre of the bubble, $\boldsymbol{e}_r = \boldsymbol{\nabla} r$ and $a(t)$ is the bubble radius. This corresponds to a pressure and deviatoric stress

$$p = C + \frac{(1-n)\eta_0 12^{(n+1)/2} a^{2n} |\dot{a}|^{n-1} \dot{a}}{3n r^{3n}}, \quad \tau_{rr} = -\frac{4\eta_0 12^{(n-1)/2} a^{2n} |\dot{a}|^{n-1} \dot{a}}{r^{3n}},$$

for some $C(t)$. If p is averaged over a region between $r = a$ and $r = a/\alpha^{1/3}$, then the average pressure is found to be

$$\bar{p} = C + \frac{\eta_0 12^{(n+1)/2} |\dot{a}|^{n-1} \dot{a}}{3n a^n} \left(\frac{\alpha^n - \alpha}{1 - \alpha} \right).$$

A stress balance on the bubble (with internal pressure p_a and surface tension γ) gives

$$p_a - p + \tau_{rr} = \frac{2\gamma}{a} \quad \text{on} \quad r = a$$

and, hence,

$$C = p_a - \frac{2\gamma}{a} - \frac{4\eta_0 12^{(n-1)/2} |\dot{a}|^{n-1} \dot{a}}{n a^n}.$$

We therefore obtain the normal stress difference as

$$-\tau_n = p_a - \bar{p} - \frac{2\gamma}{a} = \frac{\eta_0 12^{(n+1)/2} |\dot{a}|^{n-1} \dot{a}}{3n a^n} \left(\frac{1 - \alpha^n}{1 - \alpha} \right).$$

Now, $\dot{a}$ is related to $\dot{\alpha}$ by

$$\dot{\alpha} = \frac{3\dot{a}}{a} \alpha(1 - \alpha),$$

and $\dot{\alpha}/(1-\alpha)$ may be associated with $\boldsymbol{\nabla} \cdot \boldsymbol{u}_m$. Hence τ_n may be written in the form

$$-\tau_n = \eta_0 \left(\frac{4}{3} \right)^{(n+1)/2} \left(\frac{1 - \alpha^n}{n \alpha^n (1 - \alpha)} \right) |\boldsymbol{\nabla} \cdot \boldsymbol{u}_m|^{n-1} \boldsymbol{\nabla} \cdot \boldsymbol{u}_m,$$

which implies that a suitable function $f(\alpha)$ is

$$f(\alpha) = \left(\frac{4}{3} \right)^{(n+1)/2} \left(\frac{1 - \alpha^n}{n \alpha^n (1 - \alpha)} \right). \tag{62}$$

References

[1] J Bentley, Experiments on Geometric Travelling Salesman Heuristics. *AT & T Bell Labs. Computing Science Technical Report*, No. **151**, (August 1990).

[2] D A Drew, Mathematical modelling of two-phase flow. *Ann. Rev. Fluid Mech.* **15**, 261–291, (1983).

[3] A C Fowler, *Mathematical Models in the Applied Sciences*. Cambridge, (1997).

[4] S A Roach, *The Theory of Random Clumping*. Methuen, (1968).

[5] M D Penrose, On a continuum percolation model. *Advances in Applied Probability* **23**, 536–556 (1991).

[6] R Meester and R Roy, *Continuum Percolation*. Cambridge University Press, (1996).

[7] J Quintanilla and S Torquato, Clustering in a continuum perclation model. *Advances in Applied Probability* **29**, 327–336 (1997).

[8] M D Penrose, *Random Geometric Graphs*. Oxford University Press, (2003).